2021 43rd Annual International Conference of the
IEEE Engineering in Medicine & Biology Society (EMBC)
Oct 31 - Nov 4, 2021. Virtual Conference

Transcutaneous Energy Transmission System for a Totally Implantable Artificial Heart Using a Two-Wire Archimedean Spiral Coil

Tomoki Okinaga, Takahiko Yamamoto and Kohji Koshiji, *Member, IEEE*

Abstract— **This paper describes the application of a proposed spiral coil to the transformer of a transcutaneous energy transfer system for a totally implantable artificial heart. To reduce the number of rectifier components in the power receiving circuit, the shape of the power receiving transformer was reviewed. The results indicated that the power transmission efficiency between the transformers was almost the same as that of the receiving transformer with the same shape. In addition, the calculations indicated that the power transmission efficiency including that of the power receiving circuit was increased, and the number of components in the power receiving circuit was reduced.**

Keywords—artificial heart, spiral coil, center tap, inductive power transfer, rectifying circuit.

I. Introduction

Heart transplantation is performed to treat serious heart diseases [1], [2]. However, it is difficult to secure a sufficient number of hearts for transplantation. To address this, artificial heart implantation using cables to transmit power through the skin inside and outside the body is currently being clinically proposed [3]-[5]. However, this means that the patient is exposed to a risk of infection at the site of cable invasion or can suffer due to problems such as cable breakage. In order to solve these problems and improve the patient's quality of life (QOL), a transcutaneous energy transmission system (TETS) [6]-[9] has been proposed as a reliable system that does not require any cables for power transmission.

The TETS has a power receiving circuit implanted in the body for power transmission; thus, it is necessary to reduce the size of this power receiving circuit. However, general bridge full-wave rectification requires a large number of components in the rectifier, which increases the mounting volume of the board. Although half-wave rectification is an alternative solution to this problem, the ripple ratio becomes twice as large when using the same smoothing circuit as for full-wave rectification. This can be addressed by doubling the value of the smoothing capacitor, but this causes a large inrush current to flow when the power is turned on. This leads to an increase in the number of components for further failure protection. Owing to the problems that can occur with each rectification method, the center-tap full-wave rectification method is preferred over the others. In these systems, called externally coupled transcutaneous energy transmission systems [10], [11], a part of the skin is molded into a ring to match the shape of the core of the receiving coil. An externally coupled coil is magnetically coupled to the ring, and power is transmitted without invading the inside or outside of the body. However, there are only a few reports of this system because it significantly damages the appearance of the patients. Currently, a thin flat plate coil such as a spiral coil is mainly used for this method [12], [13]. Although this method does not compromise the appearance of patients, the general shape of the spiral coil makes rectification using a center tap impossible.

In this paper, we propose a TETS that uses a two-wire Archimedean spiral coil (TASC) as a power receiving coil. The proposed TETS solves the following two problems of TETSs using a spiral coil for power reception.

1) Maintaining the function of the full-wave rectifier circuit while reducing the number of components.

2) Realizing a center-tap rectifier circuit without damaging the visual appearance of the patients.

To confirm these improvements, this paper first proposes the TASC and compares its characteristics with those of typical spiral coils. Next, the equivalent circuit model is used to study the power transmission. Finally, the TASC is evaluated using an actual circuit.

II. Transcutaneous Energy Transmission System

Figure 1 shows a block diagram of a typical TETS. Electric power is sent to the inverter from a direct current (DC) power source in a rechargeable battery outside the body. The power sent to the inverter is converted to a 300 kHz alternating current (AC) power source and sent to the inside of the body using a transcutaneous transformer. The transcutaneous transformer uses magnetic coupling and thus does not require any cables. The energy delivered to the body is reconverted to DC power by rectifying and smoothing circuits for ease of use.

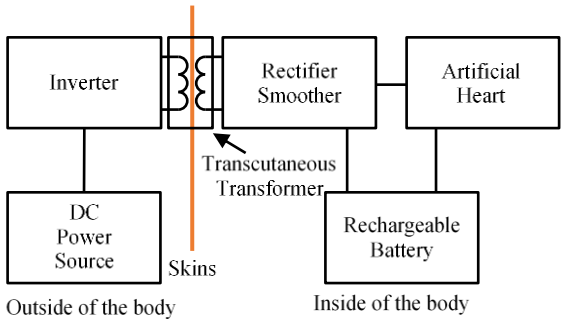

Fig. 1. Block diagram of transcutaneous energy transmission system.

*Research supported by JSPS KAKENHI Grant Number 20K12631.

T. Okinaga, T. Yamamoto and K. Koshiji are with the Department of Electrical Engineering, Graduate school of Science and Technology, Tokyo University of Science, Chiba, Japan (phone: +81-4-7124-1501; fax: +81-4-7120-1741; e-mail: t_yamamoto@rs.tus.ac.jp).

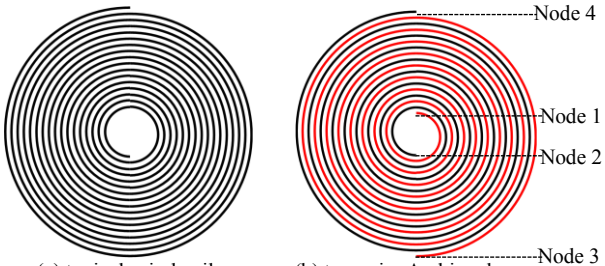

(a) typical spiral coil (b) two-wire Archimedean spiral coil

Fig. 2. Shape of typical and proposed coils.

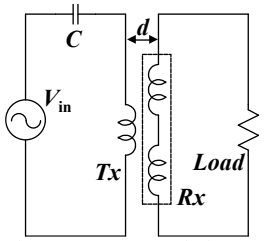

Fig. 3. Power transmission efficiency measurement circuit.

TABLE I. MEASUREMENT CIRCUIT'S PARAMETERS

Parameter	Value
V_{in}	10 V
Frequency	300 kHz
C	15.7 nF
Load	30 Ω
d	12 mm

This energy is then fed to an implanted backup battery and the actuator of an artificial heart. This study examines the transformer part.

The TETS proposed in this paper uses wireless power transmission based on magnetic resonance coupling [14]–[16]. In general, the electromagnetic induction method is used for wireless power transmission, and it is an excellent method for power transmission with a range of a few millimeters. However, a TETS cannot shorten the distance because the power is transmitted through the skin. Therefore, we adopted the magnetic resonance coupling method, which is excellent for wireless power transmission with a small coupling coefficient.

III. TWO-WIRE ARCHIMEDEAN SPIRAL COIL

A. Structure of two-wire Archimedean spiral coil

The transcutaneous transformer, which is responsible for the power transmission of the TETS, uses a spiral coil with a flat air core, as shown in Figure 2(a). The flat air-core spiral coil is suitable for implantation in the body because it does not require a large mounting volume. The proposed TASC shown in Figure 2(b) is made by winding two strands together with the same inner and outer diameters as the spiral coil shown in Figure 2(a). The TASC is designed with the same area as that of a typical flat air-core spiral coil. Therefore, it has the same advantages as those of a conventional one and can be easily replaced. The TASC can also be used as a spiral coil with a center tap by selecting and connecting two of the four nodes of the TASC.

B. Comparison of power transfer efficiency

To evaluate the performance of the TASC, we measured the power transfer efficiency when the power was transmitted from the spiral coil to the spiral coil or to the TASC. The measurement circuit is shown in Figure 3, and the parameters of the measurement circuit are listed in Table I. There are four possible ways to select the nodes of the TASC; however, as

TABLE II. MEASUREMENT CONDITIONS

Node	1	2	3	4
Position[a]	Inside	Inside	Outside	Outside
Line[a]	Red	Black	Red	Black
Case 1	Power supply to spiral coil			
Case 2	Tapped	Tapped	Open	Open
Case 3	Open	Tapped	Tapped	Open
Case 4	Open	Open	Tapped	Tapped

[a] The position and line refer to the same thing as in Figure 2(b).

TABLE III. POWER TRANSFER EFFICIENCY OF EACH CASE

Case	1	2	3	4
Power Transfer Efficiency	0.7078	0.0077	0.6995	0.0056

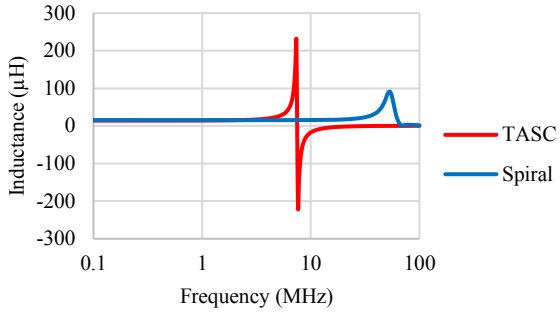

Fig. 4. Self-resonant frequency of two coils.

the two wires are wound in the same shape, the efficiency was compared between the three cases shown in Table II and the power transmission between the spiral coils. The distance between the transmission and receiving coils was set to 12 mm, which is the same as the thickness of skin, and the measurements were taken without inserting a bioequivalent phantom or a biological tissue between them. The inner diameter of the coil was 10 mm, and the outer diameter was 50 mm.

The results of the experiment are shown in Table III. The results shown in the table indicate that the difference in power transfer efficiency between the spiral coils and Case 3's TASC with one arm inside and the other arm outside is less than 0.01. The results show that the power transfer efficiency is the same for power transmission to a general spiral coil and the TASC with the nodes correctly selected. The direction of the current flow is different between Case 3 and the other cases. The spiral coil and the TASC in Case 3 have the same direction of current flowing in the neighboring conductors, but not in the other cases. We assume that this is the reason for the highly efficient power transmission.

C. Self-resonant frequency

The TASC has a larger parasitic capacitance between the windings than the spiral coils owing to its structure. This leads to a lower self-resonant frequency; therefore, if the transmission frequency is shifted due to misalignment or stray capacitance with the human body, it may behave unexpectedly. The spiral coil was fabricated with the same inner and outer diameters and the same total number of turns of the two wires as the TASC, and the self-resonant frequency was measured together with the TASC, as shown in Figure 4.

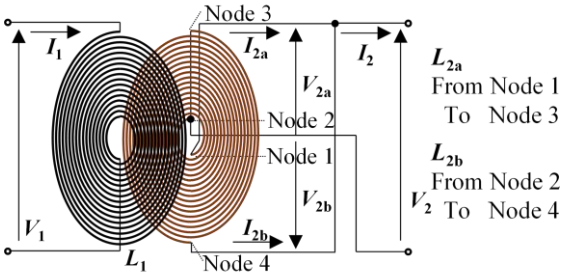

Fig. 5. Power transmitting circuit using a center-tapped coil.

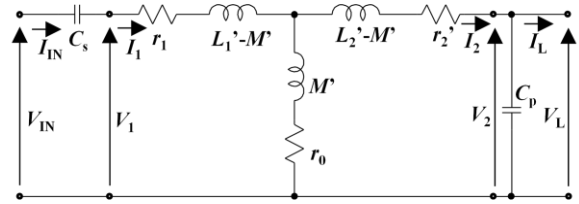

Fig. 6. T-shaped equivalent circuit.

Figure 4 shows that the self-resonant frequency of the TASC is lower than that of the spiral coil; however, the inductance does not change significantly around 300 kHz. Thus, the TASC can be used at the same frequency as before.

IV. Circuit Analysis and Measurement

Wireless power transmission to artificial hearts should be efficient. In Section III, the power transfer efficiency between the coils was derived by measurement, but the power transfer efficiency changed considerably when the rectifier components and smoothing circuit were included. Therefore, the power receiving circuit was designed to improve the power transfer efficiency when the TASC was used.

A. Equivalent circuit modeling

There are several reasons for the reduced power transfer efficiency, but one of the prime reasons is the power consumption in the rectifier component. This consumption causes heat generation, which is a major issue for systems with power-receiving circuits implanted in the body. We are attempting to analyze the circuit using calculations; however, the analysis of the circuit with center taps is complicated and requires a long time. In this section, we will convert the center-tapped rectifier circuit into a T-shaped equivalent circuit to make it easier to draw comparisons with the bridge full-wave rectifier circuit.

A schematic of the power transmission from the power feed spiral coil to the power-receiving TASC is shown in Figure 5. Although this is not shown in the figure, L_1, L_{2a}, and L_{2b} include the winding resistors r_1, r_{2a}, and r_{2b}. The circuit equation for Figure 5 can be expressed as (1).

$$\begin{bmatrix} V_1 \\ V_{2a} \\ V_{2b} \end{bmatrix} = j\omega \boldsymbol{L} \begin{bmatrix} I_1 \\ I_{2a} \\ I_{2b} \end{bmatrix} = j\omega \begin{bmatrix} L_1 & M_{12a} & M_{12b} \\ M_{12a} & L_{2a} & M_{2a2b} \\ M_{12b} & M_{2a2b} & L_{2b} \end{bmatrix} \begin{bmatrix} I_1 \\ I_{2a} \\ I_{2b} \end{bmatrix} \quad (1)$$

The TASC connections shown in Figure 5 can be considered to be connected in parallel to the ground voltage. By using admittance to simplify future calculations, (1) can be rearranged using the remainder factor, as shown in (2).

$$j\omega \begin{bmatrix} I_1 \\ I_{2a} \\ I_{2b} \end{bmatrix} = \boldsymbol{L}^{-1} \begin{bmatrix} V_1 \\ V_{2a} \\ V_{2b} \end{bmatrix} = \frac{1}{|\boldsymbol{L}|} \begin{bmatrix} \Delta_{11} & \Delta_{21} & \Delta_{31} \\ \Delta_{12} & \Delta_{22} & \Delta_{32} \\ \Delta_{13} & \Delta_{23} & \Delta_{33} \end{bmatrix} \begin{bmatrix} V_1 \\ V_{2a} \\ V_{2b} \end{bmatrix} \quad (2)$$

As explained in Section III-B, the two wires of the TASC are wound in the same shape. In this case, the inductance of each wire is ideally the same, so the current flowing and the voltage applied are also the same. Thereafter, $L_2 = L_{2a} = L_{2b}$, $r_2 = r_{2a} = r_{2b}$, $M_{12} = M_{12a} = M_{12b}$, $V_2 = V_{2a} = V_{2b}$, and $I_2 = I_{2a} = I_{2b}$. We do not derive r_0 in this study because it is not used in the derivation of power transfer efficiency.

Figure 6 shows the T-shaped equivalent circuit of Figure 5 with resonant capacitors inserted and the corresponding parameters. The circuit equation of Figure 6 can be expressed as (3) using the remainder factor in (2).

$$j\omega \begin{bmatrix} I_1 \\ I_2 \end{bmatrix} = \frac{1}{|\boldsymbol{L}|} \begin{bmatrix} \Delta_{11} & \Delta_{21} + \Delta_{31} \\ \Delta_{12} + \Delta_{13} & \Delta_{22} + \Delta_{23} + \Delta_{32} + \Delta_{33} \end{bmatrix} \begin{bmatrix} V_1 \\ V_2 \end{bmatrix} \quad (3)$$

(3) can be expressed in terms of voltage as in (4). From (4), the values of self-inductance L_1', L_2', and mutual inductance M' in Figure 6 can be expressed as (5) using the parameters shown in Figure 5.

$$\begin{bmatrix} V_1 \\ V_2 \end{bmatrix} = j\omega \boldsymbol{L_p} \begin{bmatrix} I_1 \\ I_2 \end{bmatrix} = j\omega \begin{bmatrix} L_1' & M' \\ M' & L_2' \end{bmatrix} \begin{bmatrix} I_1 \\ I_2 \end{bmatrix} \quad (4)$$

$$\begin{cases} L_1' = L_1 \\ L_2' = \left(L_2 + M_{2\alpha 2\beta}\right)/2 \\ M' = M_{12} \end{cases} \quad (5)$$

The other parameters, r_2', C_s, and C_p in Figure 6, were also obtained by using the parameters derived in Figure 5 and Figure 6, as an addition to the angular frequency ω_0 and the coupling coefficient k between the transmission spiral coil and receiving TASC.

$$r_2' = r_2/2 \quad (6)$$

$$C_p = 1/\omega_0^2 L_2' \quad (7)$$

$$C_s = 1/\omega_0^2 L_1'(1 - k^2) \quad (8)$$

B. Comparison of power transfer efficiency

The inductance and coupling coefficients of the transmission spiral coil and the receiving spiral coil and TASC used in Section III-B were measured. The results were substituted into (5) to (8), and the circuit was built based on the obtained values. A bridge rectifier circuit was used for the circuit using the spiral coil as the receiving coil, and a center-tap rectifier circuit was used for the circuit using the TASC. A full-wave rectifier circuit is preferred to reduce the ripple. The spiral coil requires four diodes to achieve this, but the TASC is tapped, so it is possible to achieve this with only two of them.

TABLE IV. MEASUREMENT CIRCUIT'S PARAMETERS

Parameter	Value	Parameter	Value
V_{in}	10 V	d	12 mm
Frequency	300 kHz	M'	5.43 μH
C_s	21 nF	L_2'	13.2 μH
r_1	100 mΩ	r_2'	50 mΩ
L_1'	15.6 μH	C_p	21 nF

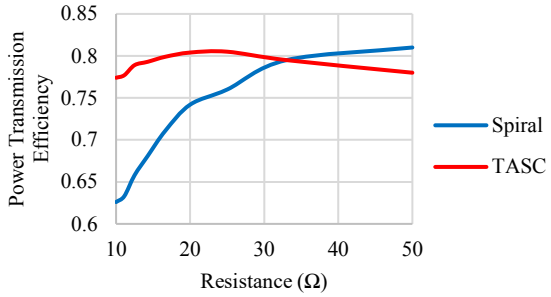

Fig. 7. Comparison of power transfer efficiency by measurement.

The derived parameters are listed in Table IV. In this study, the power transfer efficiency was measured by varying the load resistance from 10 Ω to 50 Ω, assuming that the HVAD [17] is fed with power. A value of 10 Ω corresponds to a very large load resistance when the HVAD is turned on, but the rated load resistance is designed to be 33 Ω. According to the measurement results shown in Figure 7, the TASC is more efficient from 10 Ω to 33 Ω, while the spiral coil is more efficient for higher load resistances. At the assumed value of load resistance of the HVAD, the TASC was more efficient, and even when the load resistance became lower, the TASC was able to maintain a high efficiency of over 77%.

V. CONCLUSIONS

In this paper, we discussed a transcutaneous energy transmission system using a two-wire Archimedean spiral coil. We showed that the proposed coil could be fabricated to be as thin as a typical spiral coil, thereby not affecting the visual appearance of the patient. Our measurements also showed that the proposed coil is capable of highly efficient power transmission with an efficiency greater than 77% over the range of load resistances considered for use.

References

[1] J. Stehlik, J. Kobashigawa, S. A. Hunt, H. Reichenspurner and J. K. Kirklin, "Honoring 50 Years of Clinical Heart Transplantation in Circulation," Circulation, vol. 137, no. 1, 2018, pp. 71- 87.

[2] C. Harris, C. Cao, B. Croce and S. Munkholm-Larsen, "Heart transplantation," Ann. Cardiothoracic Surg., vol. 7, no. 1, 2018, p. 172.

[3] J. A. Cook, K. B. Shah, M. A. Quader, R. H. Cooke, V. Kasirajan, K. K. Rao, M. C. Smallfield, I. Tchoukina and D. G. Tang, "The total artificial heart," Journal of Thoracic Disease, vol. 7, no. 12, 2015, pp. 2172-2180.

[4] S. F. Perrodin, O. Muller, F. Gronchi, L. Liaudet, R. Hullin and M. Kirsch, "Extracorporeal total artificial heart as bailout surgery," Journal of Cardiac Survey, vol. 32, no. 3, 2017, pp. 222-228.

[5] H. Kato and S. K. Gandhi, "Use of Berlin Heart ventricular assist devices as a total artificial heart," The Journal of Thoracic and Cardiovascular Surgery, vol. 156, no. 2, 2018, pp. 743-745.

[6] I. Hashimoto and K. Shiba, "Analysis of low leakage magnetic field transcutaneous energy transfer for ventricular assist devices," 2015 IEEE Biomedical Circuits and Systems Conference (BioCAS), 2015, pp. 45-48.

[7] T. D. Dissanayake, D. M. Budgett, P. Hu, L. Benne, S. Pyner, L. Booth, S. Amirapu, Y. Wu and S. C. Malpas, "A Novel Low-Temperature Transcutaneous Energy Transfer System Suitable for High Power Implantable Medical Devices: Performance and Validation in Sheep", J Artificial organs, vol. 34, no. 5, 2010, pp. E160-E167.

[8] T. Seshimo, T. Yamamoto and K. Koshiji, "Downsizing of Coreless Coils for Transcutaneous Energy Transmission in Implantable Devices - Improvement of Coupling Factor and Efficiency between Coils," The 35th Annual International Conference of the IEEE Engineering in Medicine and Biology Society, 2013, pp. 1871-1874.

[9] T. Okinaga, T. Yamamoto and K. Koshiji, "Reduction of surge voltage in transcutaneous energy transmission system using half-active rectifier," The 8th Meeting of the International Federation for Artificial Organs, vol. 48, no. 2, 2019, p. 166.

[10] T. Yamamoto, K. Koshiji, K. Tsukahara, E. Tatsumi, Y. Taenaka, H. Takano and K. Shiba, "An Externally-coupled Transcutaneous Energy Transmission System for Totally Implantable Artificial Hearts - Detection of Abnormal Coupling Caused by Misalignment and Air Gap in the Ferrite Core Junction of the Transcutaneous Transformer", Trans. of Japanese Society for Medical and Biological Engineering, vol. 43, no. 2, pp. 261-267, 2005.

[11] T. Shibuya and K. Shiba, "Externally-coupled transcutaneous energy transmission for a ventricular assist device-Miniaturization of ferrite core and evaluation of biological effects around the transformer," 2013 IEEE Biomedical Circuits and Systems Conference (BioCAS), 2013, pp. 206-209.

[12] A. Enssle, J. Heinrich and N. Parspour, "Analytical procedure for dimensioning transcutaneous inductive energy transfer systems," 2017 Brazilian Power Electronics Conference (COBEP), 2017, pp. 1-5.

[13] S. Nagato, W. Hijikata and T. Shinshi, "Evaluation of a transcutaneous energy transmission system with a flexible coil for an implantable ventricular assist device," 2017 IEEE Wireless Power Transfer Conference (WPTC), Taipei, 2017, pp. 1-3.

[14] T. Imura and Y. Hori "Maximizing Air Gap and Efficiency of Magnetic Resonant Coupling for Wireless Power Transfer Using Equivalent Circuit and Neumann Formula", IEEE Transactions on Industrial Electronics, vol. 58, no. 10, 2011, pp. 4746-4752.

[15] T. C. Beh, M. Kato, T. Imura, S. Oh and Y. Hori, "Automated Impedance Matching System for Robust Wireless Power Transfer via Magnetic Resonance Coupling," IEEE Transaction on Industrial Electronics, vol. 60, no. 9, 2013, pp. 3689-3698.

[16] V. Jiwariyavej, T. Imura and Y. Hori, "Coupling Coefficients Estimation of Wireless Power Transfer System via Magnetic Resonant Coupling using Information from Either Side of the System," IEEE Journal of Emerging and Selected Topics in Power Electronics, vol. 3, no. 1, 2015, pp. 191-200.

[17] Ventricular Assist Devices - Heartware HVAD System | Medtronic, https://www.medtronic.com/us-en/healthcare-professionals/products/cardiac-rhythm/ventricular-assist-devices/heartware-hvad-system.html, accessed Jan. 4th, 2021.